

Solving Footstep Planning as a Feasibility Problem using L1-norm Minimization

Daeun Song¹, Pierre Fernbach², Thomas Flayols², Andrea Del Prete³, Nicolas Mansard²
Steve Tonneau⁴, and Young J. Kim¹

Abstract—One challenge of legged locomotion on uneven terrains is to deal with both the *discrete problem* of selecting a contact surface for each footstep and the *continuous problem* of placing each footstep on the selected surface. Consequently, footstep planning can be addressed with a Mixed Integer Program (MIP), an elegant but computationally-demanding method, which can make it unsuitable for online planning. We reformulate the MIP into a cardinality problem, then approximate it as a computationally efficient ℓ_1 -norm minimisation, called SL1M. Moreover, we improve the performance and convergence of SL1M by combining it with a sampling-based root trajectory planner to prune irrelevant surface candidates.

Our tests on the humanoid Talos in four representative scenarios show that SL1M always converges faster than MIP. For scenarios when the combinatorial complexity is small (< 10 surfaces per step), SL1M converges at least two times faster than MIP with no need for pruning. In more complex cases, SL1M converges up to 100 times faster than MIP with the help of pruning. Moreover, pruning can also improve the MIP computation time. The versatility of the framework is shown with additional tests on the quadruped robot ANYmal.

Index Terms—Humanoid and Bipedal Locomotion, Legged Robots, Motion and Path Planning

I. INTRODUCTION

Footstep planning consists of computing a sequence of surface positions where a legged robot should step on to reach the desired goal position. It is thus a crucial problem for legged locomotion.

Footstep planning can be characterised by its combinatorial aspect. The parts of the environment where the footsteps can be placed (contact surfaces) are often disjoint. Thus a discrete choice of a surface must be made. This choice has an impact on all future footstep locations, as they are constrained relative to each other by non-linear kino-dynamic constraints. This means that the discrete choices of contact surfaces must be considered simultaneously for all footsteps.

Several relaxations have been proposed to practically address the problem of footstep planning. The model size can be reduced by approximating the robot with a point

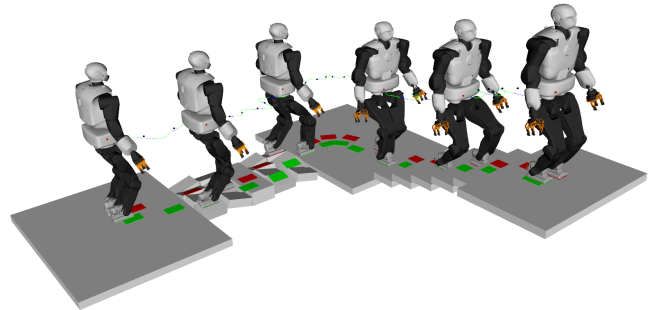


Fig. 1. A contact sequence generated by our convex-relaxed approach with domain-specific information. Talos robot is executing a planned locomotion.

mass model [1], [2], [3] and expressing the constraints as simplified functions of the Center of Mass (COM) and contact positions only [4], [5], [6]. The price for these approximations is paid with the loss of completeness [7], [8] and/or the guarantees of convergence [9], [10], [11]. What part of the problem can be approximated is thus a fundamental question, closely related to the issue of modeling the combinatorics. Discrete approaches embrace the discrete nature of the problem [12], [13], [14], [15] while continuous, optimisation-based formulations have to design strategies to handle the discrete variables. In [16], a continuation method is employed to first solve a simplified version of the problem, before using the solution as a starting point, for a more complex problem, repeating the process until the original problem is solved. Another option is to implicitly represent the discrete variables with continuous ones and to approximate the environment as a continuous function [9]. Alternatively, complementarity constraints can be used to enforce contact decisions, resulting in a computationally-demanding, non-smooth optimization problem [17], [18].

Though often conflicted in the literature, discrete and continuous approaches can be reunited in the Mixed-Integer Programming (MIP) formalism [19], [20], [21], [22], [23]. Internally, MIP solvers first solve an approximated problem, in which they relax the discrete (integer) variables into continuous ones. In the best-case scenario, the relaxed variables are converged to integer values and the original problem is solved. Otherwise, the combinatorial problem has to be addressed with branch-and-bound strategies. In the worst case, this requires solving an optimisation problem for every possible combination of values for the integer variables. Fortunately, this is rarely needed in practice, because effi-

Corresponding author: Young J. Kim.

¹D. Song and Y. J. Kim are with the Department of Computer Science and Engineering, Ewha Womans University, Seoul 03760, South Korea daeunsong@ewhain.net, kimy@ewha.ac.kr

²P. Fernbach, T. Flayols and N. Mansard are with the CNRS, LAAS, Université de Toulouse, Toulouse 31400, France pfernba@laas.fr, tflayols@laas.fr, nmansard@laas.fr

³A. Del Prete is with the Department of Industrial Engineering, University of Trento, Via Sommarive 9, Trento 30123, Italy andrea.delprete@unitn.it

⁴S. Tonneau is with the University of Edinburgh, IPAB, Edinburgh EH8 9YL, U.K. stonneau@ed.ac.uk

cient approaches exist to solve only a small fraction of the combinations [24].

In the best case, solving MIP is thus computationally equivalent to solving a continuous formulation of the problem where no specific scheme is required to address the combinatorics. From this perspective, our research question is: *is it always possible to end up with a best-case scenario for the MIP in the context of footstep planning?* A positive answer would imply that the problem can be addressed effectively by off-the-shelf optimisation solvers, resulting in simpler and faster formulations of the contact planning problem. In this paper, we empirically show that the answer is yes for a diverse range of instances of the contact planning problem, featuring stairs, rubbles, and narrow passages.

This paper is an extension of our earlier work [25] where we proposed a convex relaxation of the MIP approach for footstep planning with an ℓ_1 -norm minimization, SLIM. In this preliminary work [25], SLIM has been shown to converge to integer solutions for “simple” problems, but fails when the combinatorial complexity becomes too high (as defined in Section V). This issue is the focus of this paper.

A. Main Contributions

In this paper, we considerably improve our earlier work on SLIM by reducing the high complexity of footstep planning problems, which is to remove the non-relevant combinations of integer values from the search space. Concretely, we automatically remove integer combinations with the use of a low-dimensional path planner that computes a trajectory for the root of the robot [26]. We verified that the improved SLIM always converges to an integer solution in our test scenarios after the pruning. We experimentally validate our hypothesis that we can reach a best-case scenario for the MIP in footstep planning by pruning the irrelevant combinations.

Our main contribution is thus an LP relaxation of the MIP formulation, SLIM, experimentally shown to outperform commercial MIP solvers. Our second contribution is a demonstration that using a trajectory planner also improves the computational performance of MIP problems, especially for complex scenarios. These findings are demonstrated in several scenarios involving biped and quadruped robots navigating across uneven terrains with a pre-established gait.

II. RATIONALE

We study the combinatorial aspect of contact planning that results from environmental constraints. For instance, when climbing a staircase, we must discretely decide on which steps (or contact surfaces) our foot must land next. If we plan the next n steps and consider m possible contact surfaces for each step, the total number of possible combinations is n^m . With the MIP formalism, this means solving n^m optimisation problems in the worst case. We want to reformulate this problem so that we can find a solution by solving a single optimisation problem (or just a few).

To achieve this objective, we first recall how to write the footstep planning problem as a MIP. Then we follow two paths of action. First, we automatically reduce the number

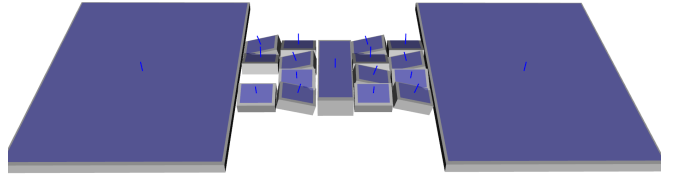


Fig. 2. A set of quasi-flat, convex surfaces (blue) configuring the environment. The blue lines indicate the normals of each surface.

of possible combinations and thus the complexity of the problem. In our staircase example, if the robot starts at the bottom of the stairs, it is useless to consider the tenth step surface when planning the very first footstep. In general, any contact surface that is not in the reachable space of the foot can be discarded from the set of candidates. We automate this pruning process with a low-dimensional sampling-based trajectory planner [27]. Second, we verify that solving a feasibility problem requires fewer iterations than solving a minimisation problem. More interestingly, after recalling that the feasibility problem can be relaxed into an ℓ_1 -norm minimisation problem, we empirically show that the relaxed problem *always* converges to a feasible solution when the combinatorics is first reduced using our trajectory.

Conversely, our results show that currently, our continuous optimisation-based formulation does not work well if an objective has to be minimised simultaneously. This issue can however be alleviated: once the contact surfaces have been selected by the ℓ_1 -norm relaxation of the feasibility problem, we can solve a second problem, which minimises a cost function but without modifying the contact surfaces selected by the first problem. This second problem boils down to a simple convex Quadratic Program (QP) [19], [25].

III. FOOTSTEP PLANNING AS A MIP

The section recalls casting the footstep planning problem as a MIP problem, slightly adapted from [25] and originally introduced in [19]. The footstep planning problem can be written as:

$$\begin{aligned}
 \text{find } & \mathbf{P} = [\mathbf{p}_1, \dots, \mathbf{p}_n] \in \mathbb{R}^{3 \times n} \\
 \text{min } & l(\mathbf{P}) \\
 \text{s.t. } & \mathbf{P} \in \mathcal{I} \cap \mathcal{G} \cap \mathcal{F} \cap \mathcal{S}^n
 \end{aligned} \tag{1}$$

We want to find a user-defined number (for now) n of footstep positions \mathbf{p}_i . Optionally we may want \mathbf{P} to minimise an objective l . \mathbf{P} must satisfy initial and goal conditions, where simple conditions can be given by the sets $\mathcal{I} : \{\mathbf{P}, \mathbf{p}_1 = \mathbf{p}_{\mathcal{I}}\}$ and $\mathcal{G} : \{\mathbf{P}, \mathbf{p}_n = \mathbf{p}_{\mathcal{G}}\}$, with $\mathbf{p}_{\mathcal{I}}$ and $\mathbf{p}_{\mathcal{G}}$ user-defined constants. The set \mathcal{F} denotes the kinematic and dynamic (here, static equilibrium) feasibility constraints that guarantee that the robot can follow the footstep plan without falling or violating joint limits. \mathcal{S} defines all the positions that lie on a surface in the environment. As a result, \mathcal{S}^n constrains all the positions of \mathbf{P} to lie on a surface.

In general, \mathcal{S} is not topologically connected, and therefore it is represented as a union of m disjoint open sets \mathcal{S}^j :

$\mathcal{S} = \bigcup_{j=1}^m \mathcal{S}^j$. In such a case, the surface constraint $\mathbf{p} \in \mathcal{S}$ is expressed as $\mathbf{p} \in \mathcal{S}^1 \cup \dots \cup \mathcal{S}^m$. We assume that the \mathcal{S}^j are quasi-flat¹, convex surfaces [28] with normal $\mathbf{n}^j \in \mathbb{R}^3$ giving the plane equation $\mathbf{p}^T \mathbf{n}^j = e^j$, with $e^j \in \mathbb{R}$ constant [19], [25] as shown in Fig. 2:

$$\mathcal{S}^j := \{\mathbf{p} \in \mathbb{R}^3 | \mathbf{S}^j \mathbf{p} \leq \mathbf{s}^j, \mathbf{p}^T \mathbf{n}^j = e^j\} \quad (2)$$

The constraints $\mathbf{p}_i \in \mathcal{S}$ can then be formulated with the use of Boolean variables:

$$\begin{aligned} \text{find } & \mathbf{p}_i \in \mathbb{R}^3 \\ & \mathbf{a}_i = [a_i^1, \dots, a_i^m] \in \{0, 1\}^m \\ & \boldsymbol{\beta}_i = [\beta_i^1, \dots, \beta_i^m] \in \mathbb{R}^m \\ \text{s.t. } & \text{card}(\mathbf{a}_i) = m - 1 \quad (3) \\ & \forall j, 1 \leq j \leq m : \quad (4) \\ & \mathbf{S}^j \mathbf{p}_i \leq \mathbf{s}^j + M a_i^j \mathbf{1} \quad (5) \\ & \mathbf{p}_i^T \mathbf{n}^j = e^j + \beta_i^j \quad (6) \\ & \|\beta_i^j\|_1 \leq M a_i^j \quad (7) \end{aligned}$$

with M being a sufficiently large constant² and $\mathbf{1}$ being a vector of appropriate size filled with ones. If $a_i^j = 0$, (7) implies that $\beta_i^j = 0$ and as a result (2) is satisfied and $\mathbf{p}_i \in \mathcal{S}_j$. If $a_i^j = 1$, then for a sufficiently large M , (5), (6), and (7) always have a solution and are effectively ignored. The cardinality function $\text{card}(\cdot)$ counts the number of non-zero entries in a vector. Therefore, (3) ensures that one contact surface is always selected.

The complete MIP formulation of our problem is thus:

$$\begin{aligned} \text{find } & \mathbf{P} = [\mathbf{p}_1, \dots, \mathbf{p}_n] \in \mathbb{R}^{3 \times n} \\ & \mathbf{A} = [\mathbf{a}_1, \dots, \mathbf{a}_n] \in \{0, 1\}^{n \times m} \\ & \boldsymbol{\beta} = [\boldsymbol{\beta}_1, \dots, \boldsymbol{\beta}_n] \in \mathbb{R}^{n \times m} \\ \text{min } & l(\mathbf{P}) \\ \text{s.t. } & \mathbf{P} \in \mathcal{I} \cap \mathcal{G} \cap \mathcal{F} \\ & \forall i, 1 \leq i \leq n : \quad (8) \\ & \text{card}(\mathbf{a}_i) = m - 1 : \\ & \forall j, 1 \leq j \leq m : \\ & \mathbf{S}_j \mathbf{p}_i \leq \mathbf{s}_j + M a_i^j \mathbf{1} \\ & \mathbf{p}_i^T \mathbf{n}^j = e^j + \beta_i^j \\ & \|\beta_i^j\|_1 \leq M a_i^j \end{aligned}$$

Assumptions

We use the following assumptions that guarantee that the MIP formulation is convex:

- l is a convex quadratic objective function.
- The contact surfaces are “quasi-flat” [28] and do not intersect with one another. This limitation is due to our dynamics constraint formulation, as explained in [25].
- Dynamic constraints are verified by computing a “quasi-static” trajectory for the center of mass (COM).

¹A surface is defined as quasi-flat when the associated friction cone contains the gravity.

²This formulation is known as the “Big M” formulation [29].

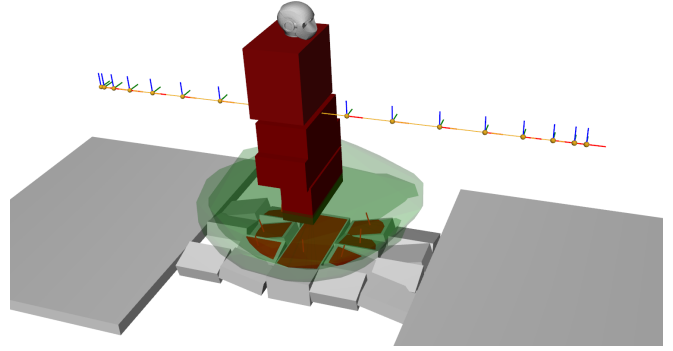


Fig. 3. Over-approximation of the reachable workspaces for the feet of Talos (green) at a given root position. The intersection between the reachable workspace of the left foot and the environment (red) defines 7 potential contact surfaces. Their normals constrain the orientation of the foot around the x- and y- axes.

- Kinematics constraints on the COM are approximated as linear inequalities.
- The gait (i.e. the contact order for the effectors) is given.
- For all \mathbf{p}_i , the orientation around the z axis of the foot in contact is given. We show how the orientation can be computed automatically in Section IV.

We can show that these assumptions define a convex feasible set \mathcal{F} for the problem. For lack of space, we refer the reader to [25] for their detailed definition.

IV. EFFICIENT REDUCTION OF THE COMBINATORICS

In (8), for each \mathbf{p}_i we consider the complete set \mathcal{S} of potential contact surfaces. However, it is reasonable to presume that for each \mathbf{p}_i only a subset $\mathcal{S}_i \subset \mathcal{S}$ of contact surfaces are feasible, because of the geometric and dynamic constraints that bind each footstep with its neighbors. We approximate the subset $\mathcal{S}_i \subset \mathcal{S}$ by exploiting the reachability condition, as introduced in [26].

A. The reachability condition

Let us assume for now that when looking for a footstep position \mathbf{p}_i , we know the position and orientation of the root of the robot $\mathbf{R}_i \in SE(3)$ at the moment when the contact is created. In this case, a necessary condition for a surface \mathcal{S}^j to be a valid candidate for \mathbf{p}_i is that \mathcal{S}^j be reachable with the foot from the root pose \mathbf{R}_i . Mathematically we can define the discrete set of reachable surfaces for footstep i as:

$$\mathcal{S}_i = \{\mathcal{S}^j \in \mathcal{S} | ROM(\mathbf{R}_i, F_i) \cap \mathcal{S}^j \neq \emptyset\}, \quad (9)$$

where F_i denotes the foot of interest, and ROM denotes the 3D range of motion of the specified foot given a specific root pose \mathbf{R}_i , which is illustrated in Fig. 3. We can scale up the ROM sufficiently to guarantee that \mathcal{S}_i contains all the potential solutions.

B. Kino-dynamic planning for estimating the root frames

In [27], we use the reachability condition to plan 6D trajectories for the root of our robot. Given the current frame \mathbf{R}_0 and a goal frame \mathbf{R}_n , we use a kino-dynamic RRT

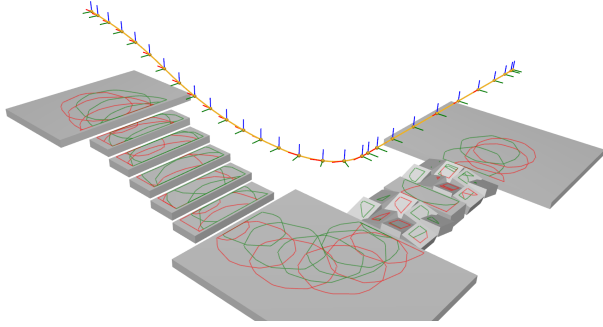


Fig. 4. Example of a planned root trajectory (yellow) with the intersected area between the ROM and the environment (red: left foot, green: right foot) at each discrete root pose. The displayed frames show the yaw (z -axis) orientation of the trajectory at the discrete points, used as the yaw orientations of the contacting feet.

planner to compute a continuous root trajectory $\mathbf{R}(t), t \in [0, T]$ of the robot, such that the reachability condition is always satisfied:

$$\forall t, \forall k, 1 \leq k \leq nFeet, ROM(\mathbf{R}(t), F_i^k) \cap S \neq \emptyset \quad (10)$$

where each F_i^k denotes one of the $nFeet$ feet of the robot. Additionally, the trajectory prevents a collision for whole-body motions computed in its neighbourhood in practice.

We discretise $\mathbf{R}(t)$ with a time step δt , which is the only hyperparameter required in our framework. Assuming a new step occurs every δt , we compute the number n of required footsteps to reach the target, as well as the estimated root poses $\mathbf{R} = [\mathbf{R}(\delta t), \mathbf{R}(2\delta t), \dots, \mathbf{R}(T)]$ at each step creation. Fig. 4 shows an example of a $SE(3)$ root trajectory and its discretisation. The reachable space of each foot is also shown for each step. We then assume that for each \mathbf{p}_i , the orientation of the foot about the z -axis is given by the z rotation of the root poses.

Using the kino-dynamic planner thus allows us to significantly reduce the number of surface candidates in our MIP problem. It is interesting to notice that the information given by the kino-dynamic planner (number of steps and rotation about the z -axis) is handled inside the quadratic cost in the MIP formulation by [19]. Their formulation presents the advantage of being self-contained, although it does not allow to consider non-flat contact surfaces, nor considers dynamic constraints. The choice of optimising the number of steps and orientation within the cost, as opposed to our potentially sub-optimal approach, deserves a discussion. We believe that the tuning required to weigh the several terms in the cost amounts to the parametrisation of the δt parameter. After all, the potential sub-optimality is the price to pay for the computational gains shown in our results, which are connected to the reduced combinatorics by our approach.

V. CONVEX RELAXATION OF THE MIP FEASIBILITY PROBLEM

We purposely formulated (8) as a special instance of what is called a *cardinality problem* [30], [31]. We observe that the constraint $\text{card}(\mathbf{a}_i) = m - 1$ constrains $\text{card}(\mathbf{a}_i)$ to its

minimum: as all the sets \mathcal{S}^j are disjoint, it is impossible for a footstep to lie simultaneously on more than one contact surface. Therefore, if we remove the cardinality constraint and replace the cost $l(\mathbf{P})$ with the term $l(\mathbf{P}) + w \sum_{i=1}^n \text{card}(\mathbf{a}_i)$, with w being a sufficiently large weight, we obtain a strictly equivalent problem.

Cardinality minimisation problems are well-known to be efficiently approximated with ℓ_1 -norm minimisation problems, thanks to the sparsity induced by the ℓ_1 -norm [32], [33]. Therefore, we replace the Boolean variables \mathbf{a}_i with the real variables α_i and minimise their norm to obtain what we call SL1M formulation [25]. Combining the ℓ_1 -norm relaxation with the pruning obtained through the use of the kino-dynamic planner as proposed in Section IV, we obtain the following problem:

$$\begin{aligned} \text{find } & \mathbf{P} = [\mathbf{p}_1, \dots, \mathbf{p}_n] \in \mathbb{R}^{3 \times n} \\ & \alpha = [\alpha_1, \dots, \alpha_n], \alpha_i \in \mathbb{R}^{+|\mathcal{S}_i|} \\ & \beta = [\beta_1, \dots, \beta_n], \beta_i \in \mathbb{R}^{+|\mathcal{S}_i|} \\ \text{min } & l(\mathbf{P}) + w \sum_{i=1}^n \sum_{j=1}^{|\mathcal{S}_i|} \alpha_i^j \\ \text{s.t. } & \mathbf{P} \in \mathcal{I} \cap \mathcal{G} \cap \mathcal{F} \\ & \forall i, 1 \leq i \leq n: \\ & \quad \forall j, 1 \leq j \leq |\mathcal{S}_i|: \\ & \quad \mathbf{S}_{i,j} \mathbf{p}_i \leq \mathbf{s}_{i,j} + M \alpha_i^j \mathbf{1} \\ & \quad \mathbf{p}_i^T \mathbf{n}_{i,j} = e_{i,j} + \beta_i^j \\ & \quad \|\beta_i^j\|_1 \leq M \alpha_i^j, \end{aligned} \quad (11)$$

where $|\mathcal{S}_i|$ is the cardinality of the set \mathcal{S}_i and $\mathbf{S}_{i,j}$, $\mathbf{s}_{i,j}$, $\mathbf{n}_{i,j}$ and $e_{i,j}$ are the constants defined for the j -th surface inside the set \mathcal{S}_i . We observe that since all the elements of α are positive, $\|\alpha_i^j\|_1 = \alpha_i^j, \forall i, j$.

For a solution of (11) to be a solution of (8), we need that $\text{card}(\alpha_i) = m - 1, \forall i$. However, this might not be the case. To handle any potential non-sparse optimum, we use a brute-force approach. We fix all the variables α_i for which the cardinality constraint is satisfied. We then test all the combinations for the remaining free variables until either i) a solution is found, ii) a maximum number of trials is reached, or iii) all possibilities are exhausted. This approach is not fail-proof, but this is a good compromise for our goal of finding a solution by solving a minimum number of optimisation problems.

An interesting observation is that because we are solving a cardinality problem, (11) is very close to the relaxed problem initially solved by a MIP solver for (8). It would be equivalent if the cardinality constraint was also reformulated as part of the cost and the pruning of contact surfaces was included in (8). In Section VI we will show that because of the preliminary operations run by a MIP solver, it is more computationally efficient to directly solve (11) if the problem converges to a feasible solution.

Extension to quadruped locomotion

In terms of discrete variables, the proposed approach extends directly to any number of legs as long as the gait is pre-defined. As such (11) and (8) remain unchanged for the quadruped robot examples demonstrated. A conservative change must however be brought in to the quasi-static constraints defining \mathcal{F} to guarantee a convex formulation. Quasi-static bipedal locomotion requires the COM to lie above the foot when the other foot breaks contact. For a quadruped, this constraint is not as limiting, as the COM can lie anywhere in the convex hull of the current contact points. However, if both the COM and feet locations are variables, the convex hull constraint is not convex. To preserve convexity, we express the COM's x and y coordinates as linear functions of the positions of the effectors (i.e. feet) in contact:

$$\mathbf{c}_{i,x,y} = \sum_k w_i^k \mathbf{p}_{i,x,y}^k, \quad \sum_k w_i^k = 1, \quad w_i^k \geq 0 \quad \forall i, \quad (12)$$

where \mathbf{p}_i^k represents the position of the k -th effectors in i -th contact, and w_i^k is a user-defined unit weighting vector that is fixed for each contact. In our tests, we set $w_i^k = 1/\text{size}(w_i)$, which results in a COM that is always in the middle of the convex hull of the contact points.

VI. EXPERIMENTAL RESULTS

We tested our approach in simulation in a variety of environments for the humanoid Talos [34] and the quadruped ANYmal [35]. To experimentally validate our framework, we provide both quantitative and qualitative comparisons against the different approaches explained, which we then discuss in Section VII. These results highlight the performance improvements thanks to the use of a trajectory to reduce the combinatorial complexity of the footstep planning problem.

A. Implementation details

The test environment is written in Python. The actual initialisation and resolution of both (8) and (11) are written in C++ and invoked through dedicated Python bindings. To provide a fair comparison, all optimisation problems are solved using the Gurobi [36] solver through those bindings³. However, open-source LP / QP solvers such as Quadprog [37] and GLPK [38] give similar performance results for the case of SL1M. This is not true for the MIP formulation. The measured computation times represent the time spent in the initialisation and resolution of the optimisation problem by the solver. The trajectory planner is implemented in the C++ HPP framework [39] and invoked from Python using a CORBA architecture. Tests were run on a PC with an AMD Ryzen 7 1700X eight-core processor on Ubuntu 18.04.

³The informed reader will observe that Python bindings already exist for Gurobi. However, the initialisation of a problem through Python is not computationally efficient, which justified the writing of a dedicated C++ library. This inefficiency also explains the difference in the computation times observed for the MIP resolution in the current work and in [25].

B. Quantitative analysis

We selected four environments representative of the difficulty of a combinatorial footstep planning problem (Fig. 5). In each scenario, the objective is to find a sequence of footsteps resulting in a feasible whole-body motion containing the given initial and goal root poses. For each scenario, we solve the footstep planning problem using three methods: MIP optimisation, MIP feasibility, and SL1M. MIP optimisation corresponds to (8), where we set an objective function, just for comparison, that minimises the difference in the distance between all footsteps. MIP feasibility and SL1M represent (8) and (11) respectively with $l(\mathbf{P}) = 0$. This means that they only solve a feasibility problem. However, once the contact surfaces are fixed, we locally optimise the footstep positions on the selected surfaces. To achieve this we call an instance of (8), where all integer variables are fixed and the quadratic cost l is reintroduced. This is a QP problem. We observe that there is no guarantee that it will converge to the optimum of the MIP optimisation formulation unless the selected contact surfaces are the same.

Additionally, each method is tested twice, either with the full combinatorics or with reduced combinatorics based on the trajectory. The same number n of footsteps is used in both cases and given by the trajectory as per Section IV.

Table I reports the computation times of each method averaged over 100 runs, together with the number of footsteps and the average number of candidate surfaces per contact. An empty cell means that the method was not able to converge to a feasible solution. In all other cases, the success rate was 100% for all the methods.

1) *Easy scenarios (bridge and stairs)*: First, we consider the environments composed of less than 10 candidate surfaces. The results show that integrating the trajectory always reduces the computation times of the optimisation problem, but the total computation time (including the guide path computation) is higher. SL1M always outperforms the other methods, being up to 7.1 times faster than MIP optimisation and up to 3.7 times faster than MIP feasibility.

2) *Hard scenarios (rubbles and rubbles & stairs)*: We also consider environments composed of more than 10 candidate surfaces, including sloped surfaces. We decided to mark SL1M without trajectory planning as a failure (blank in Table I) as the remaining combinatorics required more than 4,000 trials (Section V). Table I shows that the trajectory + SL1M configuration always converges and is also always the most computationally efficient.

The pruning improved the performance by a factor of 146.8 in the best case in the stairs & rubbles scenario with the MIP feasibility formulation. SL1M always outperforms the other methods and is up to 8.8 times faster than MIP optimisation and up to 3.1 times faster than MIP feasibility.

C. Qualitative validation

We performed whole-body motion generation using [40] to validate the computed footstep plans. Fig. 5 shows the snapshots of the generated locomotion of Talos along with the planned contact sequences for each scenario. The contact

TABLE I
CONTACT PLANNING COMPUTATION PERFORMANCE EVALUATION

Scenario	# footstep	w/o trajectory planning				w/ trajectory planning				
		# surf.	MIP opt.	MIP feas.	SLIM	avg. # surf.	trajectory	MIP opt.	MIP feas.	SLIM
bridge	16	3	157.5 ms	166.2 ms	45.3 ms	1.2	179.4 ms	87.5 ms	77.3 ms	35.5 ms
stairs	12	7	130.3 ms	59.5 ms	23.6 ms	2.0	319.0 ms	92.6 ms	34.7 ms	19.9 ms
rubbles	16	18	1914.0 ms	389.4 ms	-	5.9	252.2 ms	647.7 ms	230.2 ms	73.4 ms
rubbles & stairs	32	24	98060.5 ms	74710.5 ms	-	3.9	501.8 ms	1070.5 ms	508.9 ms	217.6 ms

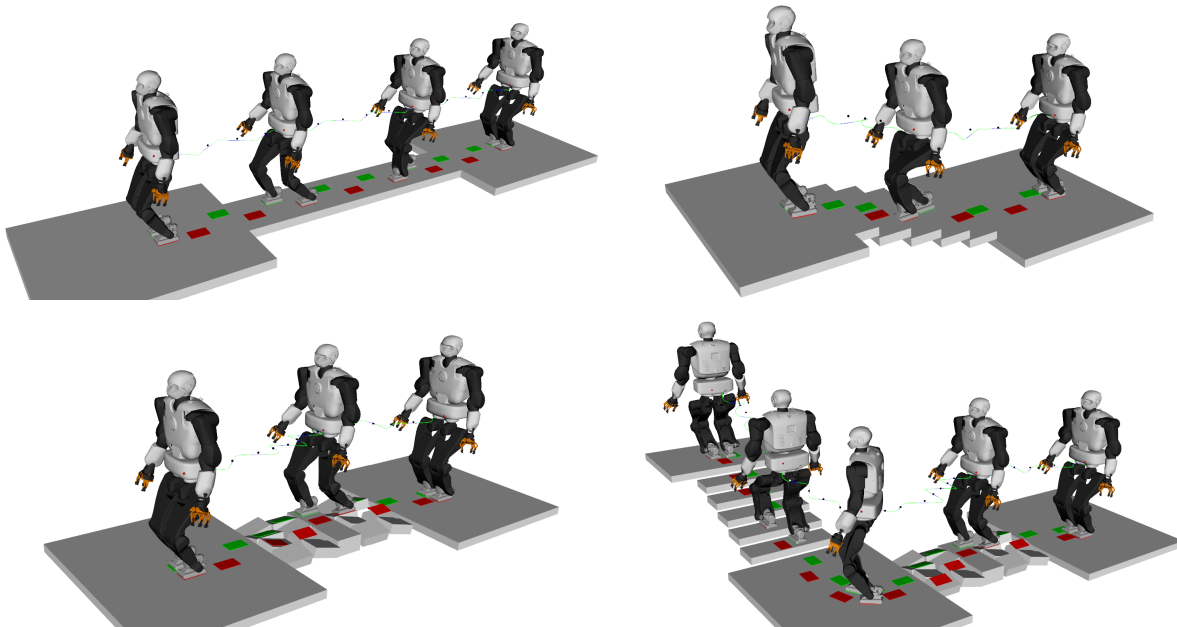


Fig. 5. Results of contact planning and the whole-body motion planning of Talos in our sample scenarios. The top row shows the *easy problems*, bridge and stairs. The bottom row shows the *challenging problems*, rubbles and rubbles & stairs.

TABLE II
COMPUTATION TIME FOR THE COMPLETE PIPELINE

Scenario	Trajectory	Footstep	Optimisation	Total
bridge	179.4 ms	35.5 ms	6.9 ms	221.8 ms
stairs	319.0 ms	19.9 ms	7.5 ms	346.4 ms
rubbles	252.2 ms	73.4 ms	8.0 ms	333.6 ms
rubbles & stairs	501.8 ms	217.6 ms	19.3 ms	738.7 ms

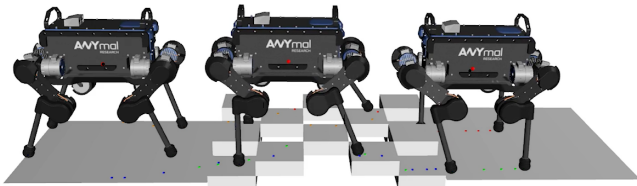


Fig. 6. Result of the contact planning and the whole-body motion planning of a quadruped, ANYmal, crossing the pallet. The colored cubes indicate the planned contact for each foot.

surfaces are selected using SLIM with the trajectory planning and then the footstep positions are optimised with a QP formulation. We also present a qualitative result obtained with the quadruped in Fig. 6. While our problem constraints ensure the existence of a quasi-static COM trajectory, the resulting motions need not be quasi-static.

D. Complete Pipeline

Table II shows the average computation time profiling the pipeline in the trajectory planner + SLIM configuration. The computation times are broken down in i) trajectory planning,

ii) contact surface selection with SLIM, and iii) QP-based footstep location optimisation.

VII. DISCUSSION

From these experiments, we draw two conclusions. First, decreasing the possible combinations with a trajectory planner reduces the computation time needed to solve the tested optimisation problems. The improvement ranged from over 146.8 times to 1.180 times and it also improved the convergence of SLIM in challenging scenarios. Pruning the non-relevant candidates was more effective in challenging scenarios than in easy scenarios with stronger reduction on the complexity ($\#surf \cdot \#footstep$) of the problem. Indeed in easy scenarios, the time required for pruning outweighed the time savings in the optimization phase. Second, solving

feasibility problems (SL1M, MIP feasibility) is faster than solving optimisation problems (MIP optimisation) in general. The performance is further improved when integrated with the trajectory planner.

A. Always use the trajectory planner

Due to the time consumption of the trajectory planner, using a trajectory is not efficient for *easy problems* in terms of computation time. However, since it brings other advantages such as automatic constraint construction and foot orientation information, we recommend always using it. Furthermore, for *hard problems*, computational gains are remarkable. For instance, in the rubbles & stairs scenario, it is more than 100 times faster when compared with MIP feasibility without the trajectory (yellow mark in Table I).

B. Non-sparse optimum handling

The ℓ_1 -norm relaxation can lead to a non-sparse optimum solution, in which case the relaxed integer variables do not converge to an integer value. The probability increases as the complexity of the problem grows. A brute-force approach to handle this non-sparse optimum normally works well with easy problems. However, with challenging problems, where the number of footsteps is large, it can result in large combinatorics, which we label as a failure. There exist some methods that enhance the sparsity of ℓ_1 -norm minimisation, such as iterative reweighting [41]. However, even though more investigation needs to be done, preliminary results suggest that this approach does not significantly improve success rates for our problem. Instead, we choose to reduce the combinatorics of the problem using trajectory pruning.

C. Combinatorial reduction in MIP problems

Before solving a combinatorial problem, MIP solvers commonly perform a “*presolve*” [24], where the problem is analysed and mathematically unfeasible solutions are removed from the search space. In this regard, our trajectory planner can be considered as a domain-specific implementation of the presolve routine.

Studying the influence of the presolve in challenging scenarios gives us some relevant insight into their combinatorics. The explored branch-and-bound node counts in MIP are shown in Table III. 0 means that MIP converged to integer values at once, before getting into a branch-and-bound phase. When the trajectory is combined and the presolve is enabled in MIP, we can see that for the feasibility problem, we directly converge to a feasible solution. This is expected, as the first iteration of the MIP is equivalent to SL1M. More interestingly, this is also the case for the MIP + optimisation scenario, where 2960 nodes had to be explored to find the optimum without the trajectory. These results suggest that for our scenarios, even when considering a cost function, *there is no combinatorics involved in the resolution of the footstep planning problem*. Studying the validity of this hypothesis is an exciting direction for future work.

TABLE III
MIP EXPLORED NODE COUNTS

Scenario	Presolve	w/o trajectory		w/ trajectory	
		MIP opt.	MIP feas.	MIP opt.	MIP feas.
rubbles	disabled	2742	383	117	1
rubbles & stairs	disabled	20542	2724	7748	1
rubbles	enabled	1	1	0	0
rubbles & stairs	enabled	2960	1	0	0

D. Parameter tuning

Our framework still requires the tuning of the discretisation step δt for the trajectory, as δt is used to infer the number of footsteps required by the motion (a new footstep is created every δt). If δt is too large, the problem can become unfeasible (not enough footsteps), while a small value might increase the complexity of the problem (more footsteps and variables), resulting in an increase in computation time and potentially a failure in the convergence of SL1M. We heuristically selected a value $\delta t = 1.0s$ for the scenarios considered, but it can differ by other situations. We believe δt plays a central role in the performance of the framework and will investigate on automatically determining its value in future work, with reinforcement learning.

E. SL1M with a cost function

The main limitation of SL1M is the risk of not converging to a feasible solution. We have demonstrated that this risk is small for feasibility problems with low combinatorics. However, using SL1M jointly with an additional objective is challenging and with the current state of our knowledge, we do not recommend doing it. However, our results show that optimising the contact locations *after* the contact surfaces are selected leads to empirically convincing results. It is worth noticing that if the contact surfaces selected by the optimal solution match those selected by SL1M, they share the exact same optimum. In any other case, the solution will only be locally optimal. However, considering the simplified models that we use for footstep planning, the notion of optimality is probably only loosely related to the optimality of the resulting whole-body motion. Therefore, the suboptimality induced by SL1M may not be critical in practice.

VIII. CONCLUSION

We presented a convex optimisation framework for planning the footsteps of a legged robot walking on uneven terrain. Our results suggest a positive answer to the question: *Can we efficiently address the combinatorics of the footstep planning problems with continuous optimisation methods?*

We showed that in our use-cases the footstep planning problem can be relaxed as an ℓ_1 -norm minimisation problem (SL1M), converging to a feasible solution when the combinatorics involves less than 10 surface candidates per footstep. Problems with larger combinatorics can be pruned thanks to a kino-dynamic planner, which outputs an approximation of the trajectory followed by the root of the robot.

The benefits of the framework were measured in terms of the computational gains (more than 100 times faster than the original Mixed-Integer Program in the best case), as well as the simplicity of the approach, which can be implemented using off-the-shelf open-source numerical solvers at the cost of losing guarantees of optimality.

Our analysis of the behaviour of MIP solvers further suggested that the combination of the kino-dynamic planner and pruning methods from the literature can potentially remove the combinatorics of the problem, even when an optimal solution is desired.

ACKNOWLEDGMENT

D. Song and Y.-J. Kim are supported in part by the ITRC/IITP program (IITP-2020-0-01460) and the NRF (2017R1A2B3012701) in South Korea. The rest of the coauthors are supported by the H2020 project Memmo (ICT-7801684).

REFERENCES

- [1] S. Kajita, F. Kanehiro, K. Kaneko, K. Fujiwara, K. Harada, K. Yokoi, and H. Hirikawa, "Biped walking pattern generation by using preview control of zero-moment point," in *2003 IEEE Int. Conf. on Robotics and Automation*, vol. 2, 2003, pp. 1620–1626 vol.2.
- [2] P. M. Wensing and D. E. Orin, "High-speed humanoid running through control with a 3d-slip model," in *2013 IEEE/RSJ International Conference on Intelligent Robots and Systems*, 2013, pp. 5134–5140.
- [3] S. Caron, A. Escande, L. Lanari, and B. Mallein, "Capturability-based pattern generation for walking with variable height," *IEEE Transactions on Robotics*, vol. 36, no. 2, pp. 517–536, Apr. 2020. [Online]. Available: <https://hal.archives-ouvertes.fr/hal-01689331>
- [4] C. Brasseur, A. Sherikov, C. Collette, D. Dimitrov, and P. Wieber, "A robust linear mpc approach to online generation of 3d biped walking motion," in *2015 IEEE-RAS 15th International Conference on Humanoid Robots (Humanoids)*, 2015, pp. 595–601.
- [5] J. Carpentier, R. Budhiraja, and N. Mansard, "Learning feasibility constraints for multicontact locomotion of legged robots," in *Proc. of Robotics: Science and Systems*, Cambridge, Massachusetts, July 2017.
- [6] S. Tonneau, P. Fernbach, A. D. Prete, J. Pettré, and N. Mansard, "2pac: Two-point attractors for center of mass trajectories in multi-contact scenarios," *ACM Trans. on Graph. (TOG)*, vol. 37, no. 5, 2018.
- [7] A. Escande, A. Kheddar, and S. Miossec, "Planning contact points for humanoid robots," *Robotics and Autonomous Systems*, vol. 61, no. 5, pp. 428–442, 2013.
- [8] P. Fernbach, S. Tonneau, O. Stasse, J. Carpentier, and M. Taïx, "C-croc: Continuous and convex resolution of centroidal dynamic trajectories for legged robots in multicontact scenarios," *IEEE Transactions on Robotics*, pp. 1–16, 2020.
- [9] A. W. Winkler, C. D. Bellicoso, M. Hutter, and J. Buchli, "Gait and trajectory optimization for legged systems through phase-based end-effector parameterization," *IEEE Robotics and Automation Letters*, vol. 3, no. 3, pp. 1560–1567, 2018.
- [10] M. Fallon, S. Kuindersma, S. Karumanchi, M. Antone, T. Schneider, H. Dai, C. P. D'Arpino, R. Deits, M. DiCicco, D. Fourie, *et al.*, "An architecture for online affordance-based perception and whole-body planning," *Joun. of Field Robotics*, vol. 32, no. 2, pp. 229–254, 2015.
- [11] J. Carpentier and N. Mansard, "Multicontact locomotion of legged robots," *IEEE Trans. on Robotics*, vol. 34, no. 6, pp. 1441–1460, 2018.
- [12] T. Bretl, "Motion planning of multi-limbed robots subject to equilibrium constraints: The free-climbing robot problem," *The International Journal of Robotics Research*, vol. 25, pp. 317 – 342, 2006.
- [13] K. Hauser, T. Bretl, J.-C. Latombe, K. Harada, and B. Wilcox, "Motion planning for legged robots on varied terrain," *The International Journal of Robotics Research*, vol. 27, no. 11-12, pp. 1325–1349, 2008.
- [14] X. B. Peng, G. Berseth, K. Yin, and M. Van De Panne, "Deeploco: Dynamic locomotion skills using hierarchical deep reinforcement learning," *ACM Trans. on Graph. (TOG)*, vol. 36, no. 4, 2017.
- [15] V. Tsounis, M. Alge, J. Lee, F. Farshidian, and M. Hutter, "Deepgait: Planning and control of quadrupedal gaits using deep reinforcement learning," *IEEE Robotics and Automation Letters*, vol. 5, no. 2, pp. 3699–3706, 2020.
- [16] I. Mordatch, E. Todorov, and Z. Popović, "Discovery of complex behaviors through contact-invariant optimization," *ACM Trans. Graph.*, vol. 31, no. 4, July 2012. [Online]. Available: <https://doi.org/10.1145/2185520.2185539>
- [17] K. Yunt and C. Glocker, "Trajectory optimization of mechanical hybrid systems using sumt," in *9th IEEE International Workshop on Advanced Motion Control, 2006*. IEEE, 2006, pp. 665–671.
- [18] M. Posa, C. Cantu, and R. Tedrake, "A direct method for trajectory optimization of rigid bodies through contact," *The International Journal of Robotics Research*, vol. 33, no. 1, pp. 69–81, 2014. [Online]. Available: <https://doi.org/10.1177/0278364913506757>
- [19] R. Deits and R. Tedrake, "Footstep planning on uneven terrain with mixed-integer convex optimization," in *2014 IEEE-RAS international conference on humanoid robots*. IEEE, 2014, pp. 279–286.
- [20] H. Dai, G. Izatt, and R. Tedrake, "Global inverse kinematics via mixed-integer convex optimization," *The International Journal of Robotics Research*, vol. 38, no. 12-13, pp. 1420–1441, 2019. [Online]. Available: <https://doi.org/10.1177/0278364919846512>
- [21] D. Driess, O. Oguz, J.-S. Ha, and M. Toussaint, "Deep visual heuristics: Learning feasibility of mixed-integer programs for manipulation planning," in *Proc. of the IEEE Int. Conf. on Robotics and Automation (ICRA)*, 2020.
- [22] B. Ponton, M. Khadiv, A. Meduri, and L. Righetti, "Efficient multi-contact pattern generation with sequential convex approximations of the centroidal dynamics," 2020.
- [23] B. Aceituno-Cabezas, C. Mastalli, H. Dai, M. Focchi, A. Radulescu, D. G. Caldwell, J. Cappelletto, J. C. Grieco, G. Fernández-López, and C. Semini, "Simultaneous contact, gait, and motion planning for robust multilegged locomotion via mixed-integer convex optimization," *IEEE Robotics and Automation Letters*, vol. 3, no. 3, pp. 2531–2538, 2017.
- [24] Gurobi, "Mixed-integer programming (mip) – a primer on the basics," <https://www.gurobi.com/resource/mip-basics>.
- [25] S. Tonneau, D. Song, P. Fernbach, N. Mansard, M. Taïx, and A. Del Prete, "S11m: Sparse l1-norm minimization for contact planning on uneven terrain," in *IEEE International Conference on Robotics and Automation (ICRA)*, 2020.
- [26] S. Tonneau, A. Del Prete, J. Pettré, C. Park, D. Manocha, and N. Mansard, "An efficient acyclic contact planner for multibot robots," *IEEE Transactions on Robotics*, vol. 34, no. 3, pp. 586–601, 2018.
- [27] P. Fernbach, S. Tonneau, A. Del Prete, and M. Taïx, "A kinodynamic steering-method for legged multi-contact locomotion," in *2017 IEEE/RSJ International Conference on Intelligent Robots and Systems (IROS)*. IEEE, 2017, pp. 3701–3707.
- [28] A. Del Prete, S. Tonneau, and N. Mansard, "Fast algorithms to test robust static equilibrium for legged robots," in *2016 IEEE Int. Conf. on Robotics and Automation (ICRA)*, 2016, pp. 1601–1607.
- [29] J. Lofberg, "Big-m and convex hulls," <http://cpc.cx/t2N>, 2012.
- [30] L. Vandenbergh and S. Boyd, "Semidefinite programming," *SIAM review*, vol. 38, no. 1, pp. 49–95, 1996.
- [31] C. Lemaréchal and F. Oustry, "Semidefinite relaxations and lagrangian duality with application to combinatorial optimization," 1999.
- [32] S. Boyd, "l1-norm methods for convex-cardinality problems," *Lecture notes*, p. 11. [Online]. Available: <http://cpc.cx/sXO>
- [33] M. J. Abdi, "Cardinality optimization problems," Ph.D. dissertation, University of Birmingham, 2013.
- [34] O. Stasse, T. Flayols, R. Budhiraja, K. Giraud-Esclasse, J. Carpentier, J. Mirabel, A. Del Prete, P. Souères, N. Mansard, F. Lamiroux, *et al.*, "Talos: A new humanoid research platform targeted for industrial applications," in *2017 IEEE-RAS 17th International Conference on Humanoid Robotics (Humanoids)*. IEEE, 2017, pp. 689–695.
- [35] M. Hutter, C. Gehring, D. Jud, A. Lauber, C. D. Bellicoso, V. Tsounis, J. Hwangbo, K. Bodie, P. Fankhauser, M. Bloesch, *et al.*, "Anymal—a highly mobile and dynamic quadrupedal robot," in *2016 IEEE/RSJ Int. Conf. on Intelligent Robots and Systems (IROS)*. IEEE, 2016, pp. 38–44.
- [36] L. Gurobi Optimization, "Gurobi optimizer reference manual," 2019. [Online]. Available: <http://www.gurobi.com>
- [37] B. A. Turlach and A. Weingessel, *quadprog: Functions to solve Quadratic Programming Problems.*, 2011, r package version 1.5-4. [Online]. Available: <http://CRAN.R-project.org/package=quadprog>
- [38] A. Makhorin, "Glpk," <http://www.gnu.org/s/glpk/glpk.html>, 2008.

- [39] J. Mirabel, S. Tonneau, P. Fernbach, A.-K. Seppälä, M. Campana, N. Mansard, and F. Lamiroux, "Hpp: A new software for constrained motion planning," in *2016 IEEE/RSJ International Conference on Intelligent Robots and Systems (IROS)*. IEEE, 2016, pp. 383–389.
- [40] P. Fernbach, S. Tonneau, O. Stasse, J. Carpentier, and M. Taïx, "C-croc: Continuous and convex resolution of centroidal dynamic trajectories for legged robots in multicontact scenarios," *IEEE Transactions on Robotics*, vol. 36, no. 3, pp. 676–691, 2020.
- [41] E. J. Candes, M. B. Wakin, and S. P. Boyd, "Enhancing sparsity by reweighted ℓ_1 minimization," *Journal of Fourier analysis and applications*, vol. 14, no. 5-6, pp. 877–905, 2008.